Int. J. Electrochem. Sci., 17 **(2022)** Article Number: 220753, doi: 10.20964/2022.07.57

International Journal of
ELECTROCHEMICAL
SCIENCE
www.electrochemsci.org

Short Communication

Effect of different coatings on friction wear performance and corrosion resistance of 40Cr steel

Yihong Zhao[1,*], *Kai Wang*[1,*], *Xujun Zhai*[2], *Minjie Shi*[1], *Fangfang Li*[1], *Chengcong Ye*[1], *Jianlei Shen*[3], *Jun Zhang*[3]

[1] School of Mechanical Engineering, Yangzhou University, Yangzhou, 225127, China.
[2] Jiangsu Agriculture & Animal Husbandry Science and Technology Vocational College, Taizhou, 225300, China.
[3] Yangzhou Metal Forming Machine Tool CO., LTD, Yangzhou, 225127, China.
[*]E-mail: yihongzhao99@sina.com, wk5962040@163.com

Received: 17 April 2022 / *Accepted:* 20 May 2022 / *Published:* 6 June 2022

Closed double-point high-speed precision press is the core equipment of intelligent equipment production line of sheet metal forming. The uneven gap between ball head and ball bowl will cause serious noise pollution. The ball bowl is usually made of brass. In order to improve the friction wear performance and corrosion resistance of the ball head and ball bowl, the ball head base material 40Cr was nitrided, TiN coating and AlCrN coating are prepared on the nitride layer by Physical Vapor Deposition. The effects of different surface treatments on friction wear performance and corrosion resistance of 40Cr steel were analyzed by scanning electron microscope, electron microscope, X-ray diffractometer, microhardness tester, friction and wear tester and GAMRY ESA410 electrochemical workstation. The results show that nitriding can improve the hardness of 40Cr steel and friction wear performance, while nitriding combined with coating can obviously improve the hardness and friction wear performance. The wear mechanism of 40Cr steel and nitride layer is mainly abrasive wear and adhesive wear. The adhesion of TiN coating and AlCrN coating is 26 N and 23 N respectively. The wear mechanism of TiN coating and AlCrN coating is mainly adhesive wear. The highest corrosion potential and the lowest corrosion current density indicate that the AlCrN coating has the best corrosion resistance, followed by the TiN coating, and the nitride layer has lower corrosion resistance than coatings but is better than 40Cr steel.

Keywords: 40Cr steel; Nitriding; TiN coating; AlCrN coating; Friction and wear; Corrosion resistance.

1. INTRODUCTION

Ball head and ball bowl are the core parts of J76-400 closed double-point high-speed precision press. Figure 1 is the assembly diagram of ball head and ball bowl of J76-400 press. When the machine works, the movement mechanism of the ball head and ball bowl is as follows: the eccentric crankshaft

drives the connecting rod fixed on the clamping seat to rotate, the ball holder drives the ball head screw to swing circumferentially around the ball bowl in the slider, and the slider is driven by the ball head screw to make linear reciprocating motion up and down. From the ball head and ball bowl movement mechanism, it is found that the rotating motion of the crank mechanism is changed to the reciprocating motion of the slider. The upper die is fixed on the slide block body, and the lower die is fixed on the workbench pad, which can complete the pressure work of the material placed between the upper and lower dies. After working for a certain period of time, uneven clearance may be produced between the ball head and ball bowl due to wear and corrosion after a certain period of operation, so it will emit abnormal noise, resulting in serious noise pollution. It also affects the performance and service life of the machine. In the actual production and application of the factory, the production cycle of the ball head is longer than that of the ball bowl, and the replacement of the ball bowl is relatively simple, so it has important practical significance to improve the wear resistance and corrosion resistance of the ball head.

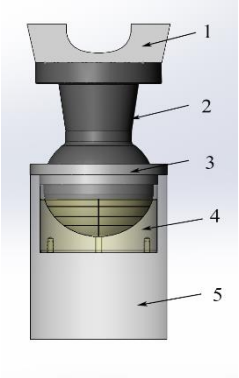

Figure 1. Schematic assembly of ball head and bowl mechanism (1. Ball holder, 2. Ball head screw, 3. Ball head pressure cover, 4. Ball bowl, 5. Slider)

The base material of the ball head is 40Cr steel, which is the most widely used alloy quenching and tempering steel in China at present. 40Cr steel is commonly used in shaft parts, important gears and connecting rod bolts and other parts[1]. 40Cr steel dosen't have very high hardness and excellent wear resistance, in order to improve the hardness and friction wear performance of 40Cr steel, surface engineering technology is an effective means. At present, there are many methods for surface engineering technology for 40Cr steel, such as surface chemical heat treatment technology, laser beam, ion beam, electron beam and other surface high energy beam surface treatment technology, electroplating, thermal spraying, hot dip surface coating technology, can improve the surface performance of parts[2-5].

Carbonitriding is a surface hardening process. In the process of gas carbonitriding, nitrogen diffused in steel not only increases hardness, but also stabilizes residual austenite and improves the surface mechanical properties of steel components[6-7]. Studies by Trojahn [8] show that carbonitrided bearings made from 100Cr6 perform much better in both clean and contaminated environment when compared to martensitic hardened 100Cr6.

Physical Vapor Deposition is the key technology to improve the wear resistance and corrosion

resistance of cemented carbide matrix. Coating under the premise of vacuum technology, clean process, high quality coating, environmentally friendly, easy to large-scale production and automatic production, can prepare a variety of coatings and multi-group composite coatings to meet different needs. TiN coating is famous for its good friction wear performance and corrosion resistance. Fan-Yi Ouyang studies effects of TiN and TiN/Ti coatings on corrosion resistance of stainless steel. The corrosion performance of the coating was tested by polarization curve and electrochemical impedance spectroscopy, and the results showed that the corrosion current of the coating with diffusion layer Ti was significantly reduced, and the barrier layer with Ti layer could effectively inhibit the charge transfer between the coating and the matrix interface and improve the corrosion resistance of the coating[9]. AlCrN coatings are particularly attractive because of their excellent oxidation resistance, chemical stability, and excellent mechanical properties[10-11].

The combination of carbonitriding and PVD can not only significantly improve the bearing capacity of the substrate surface and the bonding force between the coating and the substrate, but also improve the fatigue strength、wear resistance and corrosion resistance of the steel surface[12].For example, TiN, CrN and TiAlN Coatings with or without carbonitriding treatment were studied comparatively by J.C.A Batista [13], the results showed that double treatment had higher hardness, higher film-based adhesion and lower coefficient of friction than single coating treatment.

In this research, in order to improve the friction wear performance and corrosion resistance of 40Cr steel, the surface treatment methods of nitriding, nitriding combined with TiN coating and nitriding combined with AlCrN coating were adopted, and the microstructure and properties of 40Cr steel, nitride layer, TiN coating and AlCrN coating were compared.

2. EXPERIMENTAL

2.1 Sample Preparation

40Cr steel was used as the matrix material in the experiment, which was cut into 12 ㎜×12 ㎜ ×10 ㎜ vertical square sample by electric spark wire cutting. The sample was polished by polishing machine after being polished by metallographic sandpaper. Finally, the sample was put into anhydroethanol for ultrasonic cleaning.

Well carburizing furnace was used for nitriding treatment on the surface of the sample after cleaning. Carbon dioxide was used as the decarburizing medium, ammonia was used as the nitriding medium. The insulation temperature was 550 ℃, and the time was 5.5 h.

TiN coating and AlCrN coating were prepared by PVD1050 multi-arc ion plating machine on the surface of the sample treated by nitriding. Ti targets with high purity were selected to prepare TiN coating. When preparing AlCrN coating, Al and Cr high purity targets were selected. Argon with purity of 99.99% is selected as sputtering gas, and nitrogen with purity of 99.99% is selected as reaction gas. The flow rate of the two gases is controlled by mass flow controller.

During TiN coating preparation, the sample surface was first cleaned by ion etching for 30 min with high-energy argon gas under the control of bias voltage. Ti layer was prepared on the surface of

the sample as the bottom layer. Then a small amount of nitrogen was introduced into the vacuum chamber to reduce the bias voltage and prepare TiN transition layers. Lastly, increase nitrogen flow to prepare TiN coating coating.

When preparing the AlCrN coating, the Cr layer is prepared on the surface of the sample as the bottom layer, then the bias pressure is reduced and nitrogen is introduced, the CrN transition layer is prepared on the surface of the bottom layer, and finally the nitrogen flow rate is increased to prepare the AlCrN coating. The preparation parameters of TiN coating and AlCrN coating are shown in Table 1.

Table 1. Process parameters for perparing TiN coatings and AlCrN coatings.

Coating / Parameter	TiN	AlCrN
The background vacuum degree/pa	8.8×10-3	9.2×10-3
Substrate bias/V	80	115
Sputtering pressure/pa	2	0.5
Target current/A	140	155
Baseline temperature/℃	400	380
Deposition time/h	3	3

2.2 Characterization

The microstructure of nitride layer on 40Cr steel was observed and characterized by inverted metallographic microscope. The morphology and element composition of TiN coating and AlCrN coating were observed and characterized by field emission scanning electron microscope (FE-SEM). The crystal structure was identified by Advance Polycrystalline X-ray diffractometer, measuring angle range 30°-90°. Revetest Scratch test system (CSM Revetest) was used to test the bonding performance of the coating. In the scratch test, a diamond indener with a cone Angle of 120°, a tip radius of 0.2 ㎜, a loading speed of 5 N/s, and a scratch length of 5 ㎜ were selected. The hardness of 40Cr steel, nitride layer, TiN coating and AlCrN coating was compared by digital micro Vickers Hardness tester. The loading weight was 25 g and the holding time was 10 s.

Friction and wear testing machine was used for ball disc reciprocating dry friction and wear test, the grinding pair selected Si_3N_4 ceramic ball diameter of 4 ㎜, load 2, 4, 6 N, test speed of 40 ㎜/s, one-way sliding 5 ㎜, the test duration is 1h. 3D profilometer was used to characterize the cross section morphology of the wear marks and obtain the wear quantity, then calculate the wear rate.

GAMRY ESA410 electrochemical workstation was used to characterize corrosion resistance of four samples in 3.5 wt% NaCl solution . The sample to be tested is a working electrode, the reference electrode is a saturated calomel electrode, and the auxiliary electrode is a platinum electrode. The frequency of electrochemical impedance spectrum measurement ranges from 0.01 Hz to 10 KHz, and potentiodynamic polarization curve is measured at the scanning rate of 10 mV/s within the range of -

800 mV to -400 mV relative to the open-circuit potential.

3. RESULTS AND ANALYSIS

3.1 Micromorphology and Hardness Analysis of Nitriding Layer

Figure. 2 shows the micromorphology of the nitriding layer under metallographic microscope. It can be clearly seen that there is a white and bright layer on the surface of the sample, namely the nitride layer. The nitride layer is a compound layer, consisting of Ɛ phase, γ 'phase, ferro-nitrogen compound and carbon-nitrogen compound. Below the bright white layer is a gray-black transition layer, and the diffusion layer is formed by the dispersion of carbides, nitrides, and carbonitrides of iron and alloy elements[6]. Below the transition layer is the matrix structure. The effective thickness of nitriding layer is about 174.52μm, the thickness of nitride layer is about 14.53μm and the thickness of transition layer is about 159.99μm. It can be seen from the figure that the color of the transition layer from the bottom of the nitride layer to the top of the core matrix gradually deepened, which is due to the decomposition of ammonia under high temperature, resulting in the reaction of nitrogen atoms with 40Cr steel. The nitrogen atoms involved in the reaction first dissolve in α-Fe, and then continuously diffuse into the interior of 40Cr material, resulting in a concentration difference between the surface and the core[14].

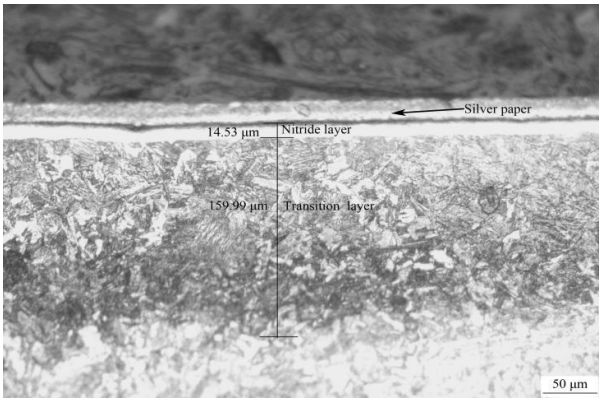

Figure 2. Microscopic morphology of the nitriding layer (Magnification: 200x)

Figure. 3 shows the hardness distribution curve of the nitriding layer, which is measured by micro-hardness tester at 20 μm intervals from the surface of the nitriding sample to the core of the sample.

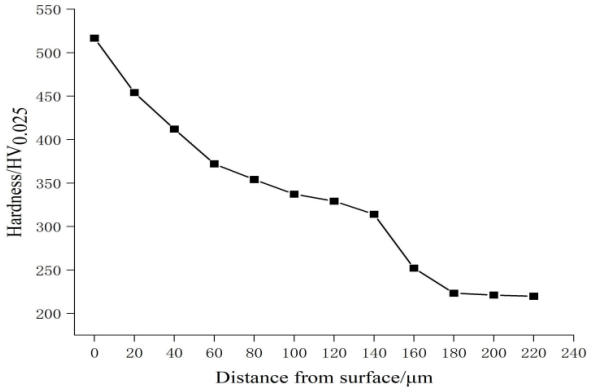

Figure 3. Hardness distribution curve of the nitriding layer. (Loading weight: 25 g; Holding time: 10 s.)

The hardness distribution curve of the nitriding layer shows an obvious gradient, and the hardness of the nitriding layer decreases with the increase of distance from the surface. The hardness of the nitride layer is the highest, reaching 516.8 $HV_{0.025}$. The transition layer is the interspace solid solution layer formed by nitrogen atoms entering into the matrix crystal[15]. The hardness of the transition layer is higher than that of the core matrix but lower than that of the nitride layer by solution strengthening. As the distance between the transition layer and the surface increases, the concentration of nitrogen atoms decreases and the solution effect weakens, so the hardness gradually decreases, and finally decreases to 223.3 $HV_{0.025}$ at 180 μm from the surface.This is also consistent with the effective nitriding layer thickness of 174.52 μm measured above.

3.2 Micromorphology and Element Distribution of TiN and AlCrN Coating

Figure. 4 shows the microscopic morphology of TiN coating and AlCrN coating, it is found that AlCrN coating has more "particles" with larger diameter than TiN coating, which are due to the evaporation of metal target under high temperature. The melted metal is deposited on the substrate surface in the form of droplet sputtering, which is a typical feature of multi-arc ion plating. However, the melting point of Ti element is higher than that of Al element, and the evaporation of Al target is more intense than that of Ti target, so more large "particles" are formed[16-17]. Table 2 shows the surface composition of TiN coating. The main components of the coating are Ti and N, which are consistent with the target material. Table 3 shows the surface composition of AlCrN coating. The main components of the coating are Al, Cr and N, among which Al atomic fraction is the highest, which can effectively improve the friction and wear performance of the coating.

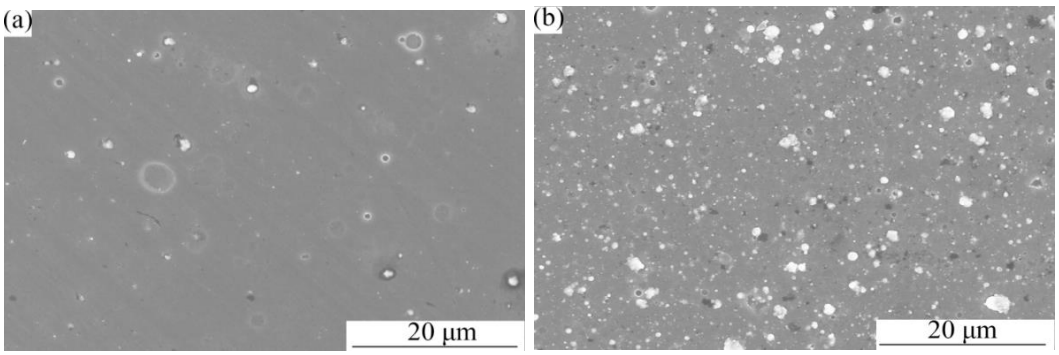

Figure 4. Surface FE-SEM morphologies of the (a) TiN coating, (b) AlCrN coating. (Magnification: 2000x)

Table 2. Elemental composition analysis of TiN coating

	Ti/%	N/%
TiN	64.85	35.15

Table 3. Elemental composition analysis of AlCrN coating

	N/%	Al/%	Cr/%	Si/%
AlCrN	26.40	48.30	22.62	2.68

Figure. 5 shows the section of TiN coating and AlCrN coating respectively. It can be seen from the figure that the coating structure is uniform and dense, and is stacked and bonded to the substrate. The measured thickness of TiN coating is about 2.7 μm, and that of AlCrN coating is about 2.3 μm.

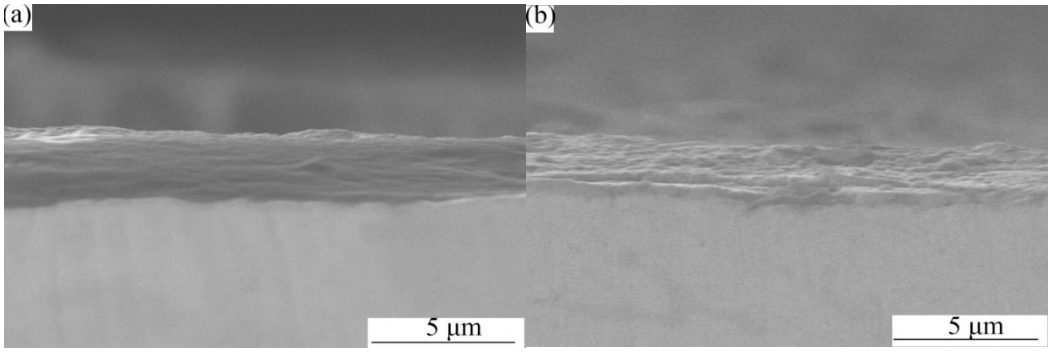

Figure 5. Cross section FE-SEM images of the (a) TiN coating, (b) AlCrN coating. (Magnification: 7000x)

3.3 XRD Analysis

Figure. 6 is the XRD phase diagram of the nitride layer, TiN coating and AlCrN coating. In Figure 6(a), the diffraction peaks of Fe (111), (200) and (211) are detected in the nitride layer. At the

same time, the diffraction peaks of (002), (110) and (111) of Fe_3N were also detected due to the solution strengthening effect of nitrogen atoms. It can be seen from Figure 6(b) that TiN coating detects diffraction peaks of TiN (111) and TiN (200) as well as diffraction peaks of Ti_2N (300). TiN (111) is the strongest peak, Ti_2N (300) is the second strongest peak and TiN (200) is the weakest. Figure 6(C) shows the diffraction peaks of CrN (111), (200) and (220) are detected by AlCrN coating, which indicates that AlCrN coating is mainly CrN phase structure with face-centered cubic structure and has a strong preferred orientation of (200) crystal surface.

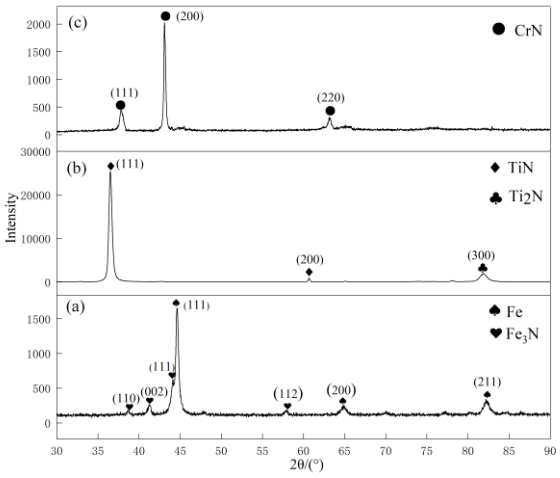

Figure 6. XRD patterns of the the (a) nitride layer, (b) TiN coating, (c) AlCrN coating. (Measuring angle range 30°-90°)

3.4 Adhesion Strength Analysis

Figure. 7 shows the adhesion strength of TiN coating and AlCrN coating. In the scratch test, the diamond indenter slowly imposes load on the coating at a speed of 5 N/s, and cracks occur on the coating surface. Finally, the coating falls off with the increase of acoustic signals, and the load when the coating falls off is the adhesion of the coating[18-19].

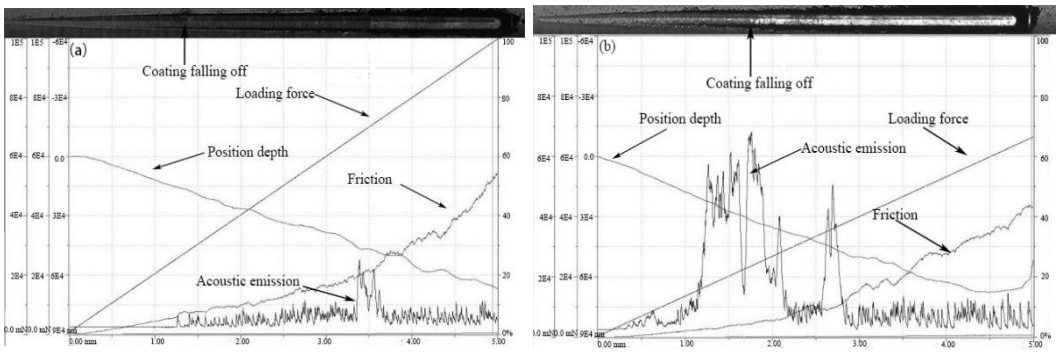

Figure 7. Test diagram of the adhesion strength of (a) TiN coating, (b) AlCrN coating. (Indenter loading speed: 5 N/s; Indentation length: 5 ㎜.)

Figure 7(a) shows us that TiN coating begins to fall off when the scratch length is 1.49 ㎜, and the load applied at this time is 26 N, that is, the adhesion of TiN coating is 26 N. It can be seen from Figure 7(b) that AlCrN coating begins to fall off at 1.79 ㎜, and the load applied at this time is 23 N, that is, the adhesion of AlCrN coating is 23 N.

3.5 Surface Hardness Analysis

Figure. 8 is the hardness contrast diagram of 40Cr sample treated by different surface treatment methods. Six points are randomly selected on the surface of 40Cr steel, nitride layer, TiN coating and AlCrN coating respectively, and the average hardness value is calculated. The average hardness value of nitride layer is 520.4 $HV_{0.025}$, which is nearly 2.4 times higher than the average hardness of 40Cr steel 217.1 $HV_{0.025}$. The average hardness of TiN coating is 1363.5 $HV_{0.025}$, which is about 6 times higher than that of matrix. The average hardness of AlCrN coating is 2856.9 $HV_{0.025}$, 13 times higher than that of matrix. The nitriding treatment makes nitrogen atoms enter the lattice gap of the 40Cr steel and plays a good role in strengthening the solution, so the nitriding treatment can effectively improve the microhardness of the matrix. The TiN coating and AlCrN coating prepared on the nitride layer can effectively improve the bearing capacity of matrix to the coating, and the composite treatment of nitriding combined with coating also forms the coating with multi-layer structure. The shear modulus of each material of the multi-layer structure coating is different, and the energy difference of the dislocation line between two adjacent layers is proportional to the shear modulus of the two materials. The dislocation must overcome this energy difference to cross the interface, so the multi-layer coating can effectively improve the microhardness[20].

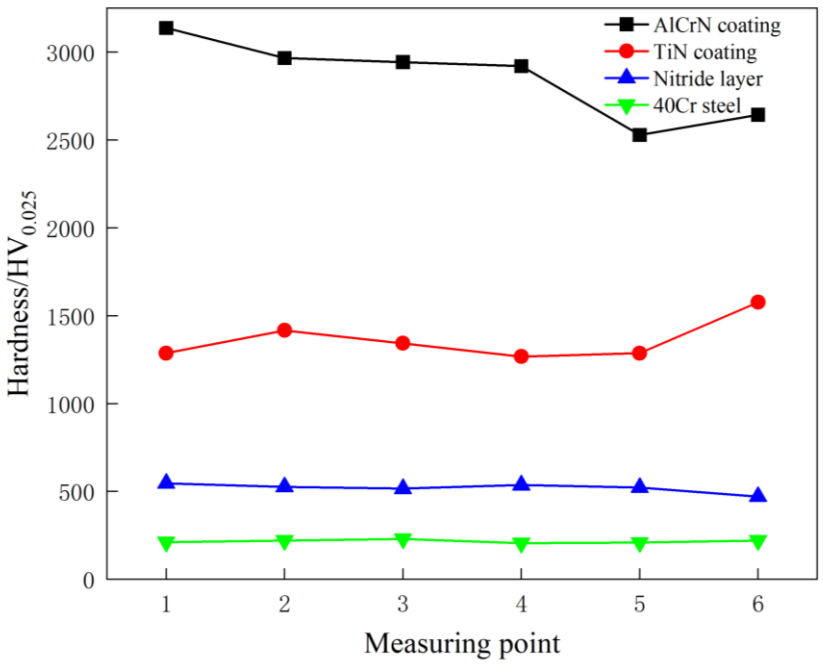

Figure 8. Hardness distribution of 40Cr samples after different treatments. (Loading weight: 25 g; Holding time: 10 s.)

3.6 Analysis of Friction and Wear Performance

Figure. 9 is the friction coefficient diagram of 40Cr steel, nitride layer, TiN coating and AlCrN coating. When the load is 2 N, 4 N and 6 N, the average friction coefficient of substrate within 1 h is about 0.72, 0.70 and 0.68, respectively.When the nitride layer is loaded at 2 N, 4 N and 6 N, the average friction coefficients within 1h are about 0.70, 0.67 and 0.64, respectively. When the load is 2 N, 4 N and 6 N, the average friction coefficient of TiN coating within 1h is about 0.65, 0.60 and 0.58, respectively.When the load is 2 N, 4 N and 6 N, the average friction coefficient of AlCrN coating within 1h is about 0.63, 0.60 and 0.59, respectively. Matrix can be seen from the Figure 9(a) in the 1200 s before the friction coefficient fluctuation is bigger, may be because the substrate surface micro convex body more, after micro convex body is smooth, Si_3N_4 ceramic ball and substrate contact area increase, increases the coefficient of friction, the friction produces in the process of wear debris, gathered a large number of wear debris will have solid lubrication[21], and can reduce the coefficient of friction, therefore, it can cause large fluctuations. Figure 9(b) shows the friction coefficient of the nitride layer rises at 500 s, which may be due to the fragmentation of the nitride layer by friction to produce hard particles[17].

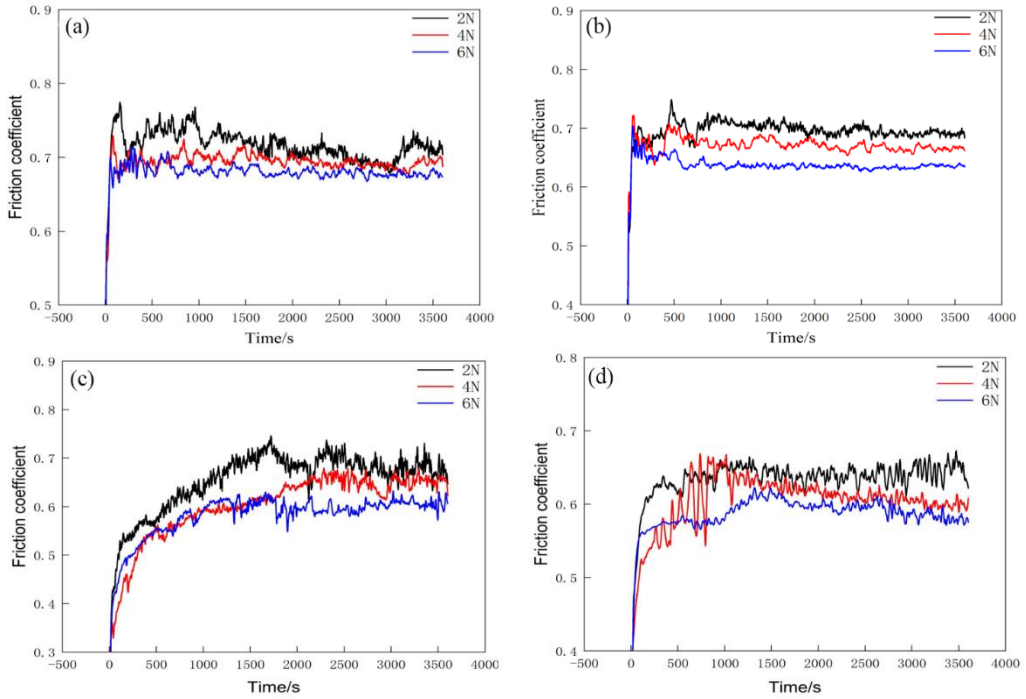

Figure 9. The friction coefficient curve of (a) 40Cr steel, (b) nitride layer, (c) TiN coating, (d) AlCrN coating. (The grinding pair selected Si_3N_4 ceramic ball diameter of 4 ㎜, load 2, 4, 6 N, test speed of 40 ㎜/s, the test duration is 1h.)

Therefore, the friction coefficient rises and enters the dynamic equilibrium stage at about 800 s. It can be seen from Figure 9(c) and Figure 9(d) that the friction coefficient of TiN coating and AlCrN coating shows an upward trend in the first 1500 s, which may be due to the fact that there are more "particles" on the coating surface. In the following 2000 s, the friction coefficient gradually enters a

dynamic equilibrium stage.AlCrN coating fluctuates greatly in the first 1000 s when the load is 4 N, which may be related to the existence of many micro-convex bodies and pits in the test area. Figures 9(a), 9(b), 9(c) and 9(d)shows us that with the increase of the test load, the friction coefficients all decline, which may be related to the oxide film generated by the temperature rise caused by the increase of the load. Compared with the 40Cr steel , the friction coefficient of the nitride layer, TiN coating and AlCrN coating decreases to a certain extent under the same load, indicating that these three surface treatment methods can improve the wear resistance of the material.

Figure. 10 shows the cross section outline of wear marks of 40Cr steel, nitride layer, TiN coating, AlCrN coating under 2 N, 4 N and 6 N loads for 1h friction, the grinding pair selected Si_3N_4 ceramic ball. The wear width of matrix increases from 90 μm to 120 μm, and the wear depth increases from 2.6 μm to 4.5 μm. The wear width of nitride layer increases from 80 μm to 100 μm, and the wear depth increases from 2.1 μm to 3.5 μm. The wear width of TiN coating increases from 50 μm to 75 μm, and the wear depth increased from 1.9 μm to 2.4 μm. The wear width of AlCrN coating increases from 60 μm to 80 μm, and the wear depth increases from 1.7 μm to 2.1 μm.

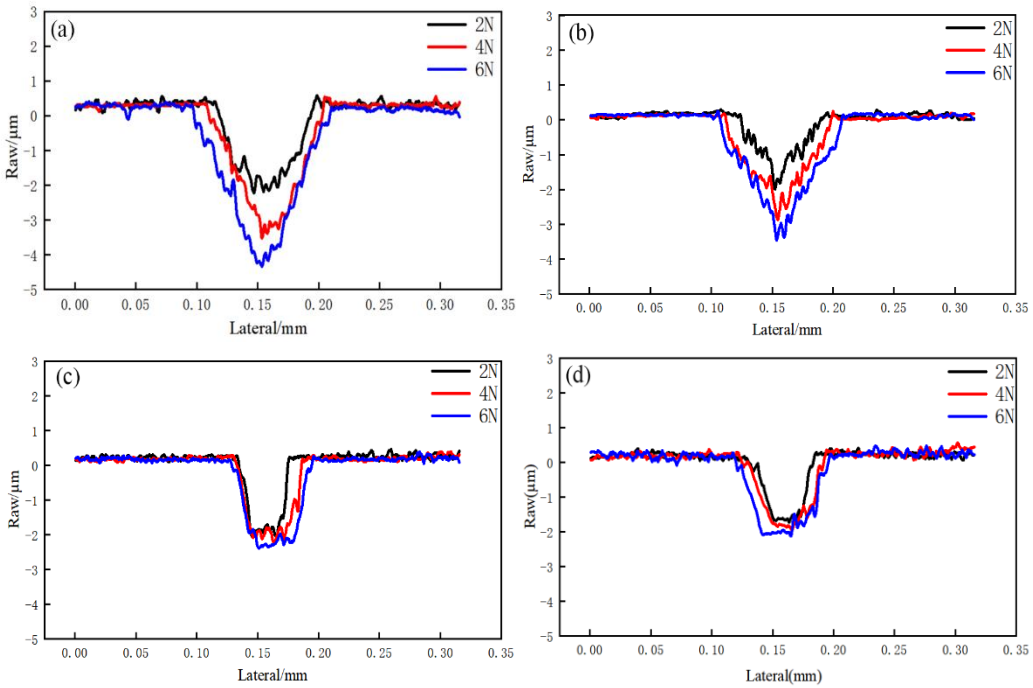

Figure 10. Wear scar profile of (a) 40Cr steel, (b) nitride layer, (c) TiN coating, (d) AlCrN coating. (The grinding pair selected Si_3N_4 ceramic ball diameter of 4 ㎜, load 2, 4, 6 N, test speed of 40 ㎜/s, the test duration is 1h.)

Contrast Figure 10 (a), 10(b), 10(c), 10(d) found nitride layer of grinding crack width narrow relative to the substrate, and the grinding crack width of TiN coating, AlCrN coating significantly narrowed, grinding crack width can characterization of plastic deformation resistance of the coating, that nitriding combined with coating surface treatment can obviously improve the ability to resist plastic deformation of materials, TiN coating is slightly better than AlCrN coating. Under the same load, the wear depth of nitride layer, TiN coating and AlCrN coating decreases to different degrees

compared with the matrix, and the AlCrN coating has the lowest abrasion depth, indicating that both nitriding and coating can improve the wear resistance of materials, and the composite treatment of nitriding combined with AlCrN coating has the best effect.

Figure. 11 shows the wear morphology of 40Cr steel, nitride layer, TiN coating and AlCrN coating. Figure 11(a), 11(b) and 11(c) show the serious plastic deformation occurs when the 40Cr steel with lower hardness is grinded against the Si_3N_4 ceramic ball with higher hardness. Due to the effect of ploughing on the surface of the 40Cr steel shear, plough wrinkling, cutting, produced along the direction of friction grooves and abrasive, abrasive also due to increased load is pressed into the surface of the 40Cr steel indentation, the material surface will also appear lamellar and scaly spalling. The greater the load, the deeper the furrows and indentations, and the more pronounced the laminar and scaly spalling. Figure 11(d), 11(e) and 11(f) show us that compared with the ball-head matrix, the wear degree of the nitride layer is lighter, and nitriding improves the hardness and wear resistance of the material. Figure 11(d) shows more hard particles are produced by the fragmentation of the nitride layer under load. As the load increases, the hard particles are ground and extruded, forming lighter massive spalling. The wear mechanism of 40Cr steel and the nitride layer is mainly abrasive wear and slight adhesive wear. As can be seen from Figures 11(g) and 11(j), when the load is 2 N, no furrows and a large number of grinding chips are formed on the surface of the coating, showing excellent wear resistance of the coating. With the increase of the load, the coating also has plastic deformation and partial shedding, and the AlCrN coating is better than TiN coating. Under 6 N load, cracks and grinding have occurred in the coating, and the crack opening is rolled up,these are given in Figure 11(I) and 11(L). After sliding friction for many times, the cracks that are rolled up are squeezed and sheared into laminar chips, and when they reach a certain size, lumps fall off and flake chips are formed. It is found that TiN coating wear is more serious and AlCrN coating wear resistance is better. EDS analysis was conducted on wear marks of TiN coating and AlCrN coating under 6 N load, and the results are shown in Table 5 and Table 6. It is found that Fe, O, Ti and Si are the main elements in area A of the analysis figure 11(I). The presence of Ti element indicates that the coating TiN is still not worn through, while Fe and O elements indicate that the oxide film containing Fe is formed, which is consistent with the increase of load and decrease of friction coefficient mentioned above. Si element comes from Si_3N_4 ceramic sphere, indicating adhesive wear. The main elements in zone B and A are the same, but the content of Ti drops and Fe increases, indicating that the coating has been basically worn out. The main elements in zone C are N, Ti and Fe, indicating that the wear here is slight and no oxide film or adhesive wear is generated. The main elements found in A zone of the analysis Figure 11(L) are coating elements Al, Cr, N and Fe, indicating that the coating has not been worn.In area B of the analysis Figure 11(L), it is found that the main elements are Al, Cr, Si, O, Fe, Al and O, indicating that Al_2O_3 film is generated, which can effectively reduce the friction coefficient and improve the friction performance[22-23]. Al and Cr elements indicate that the coating is not worn, while Si elements also indicate that the AlCrN coating also has adhesive wear. So the main wear mechanism of TiN coating and AlCrN coating is adhesive wear.

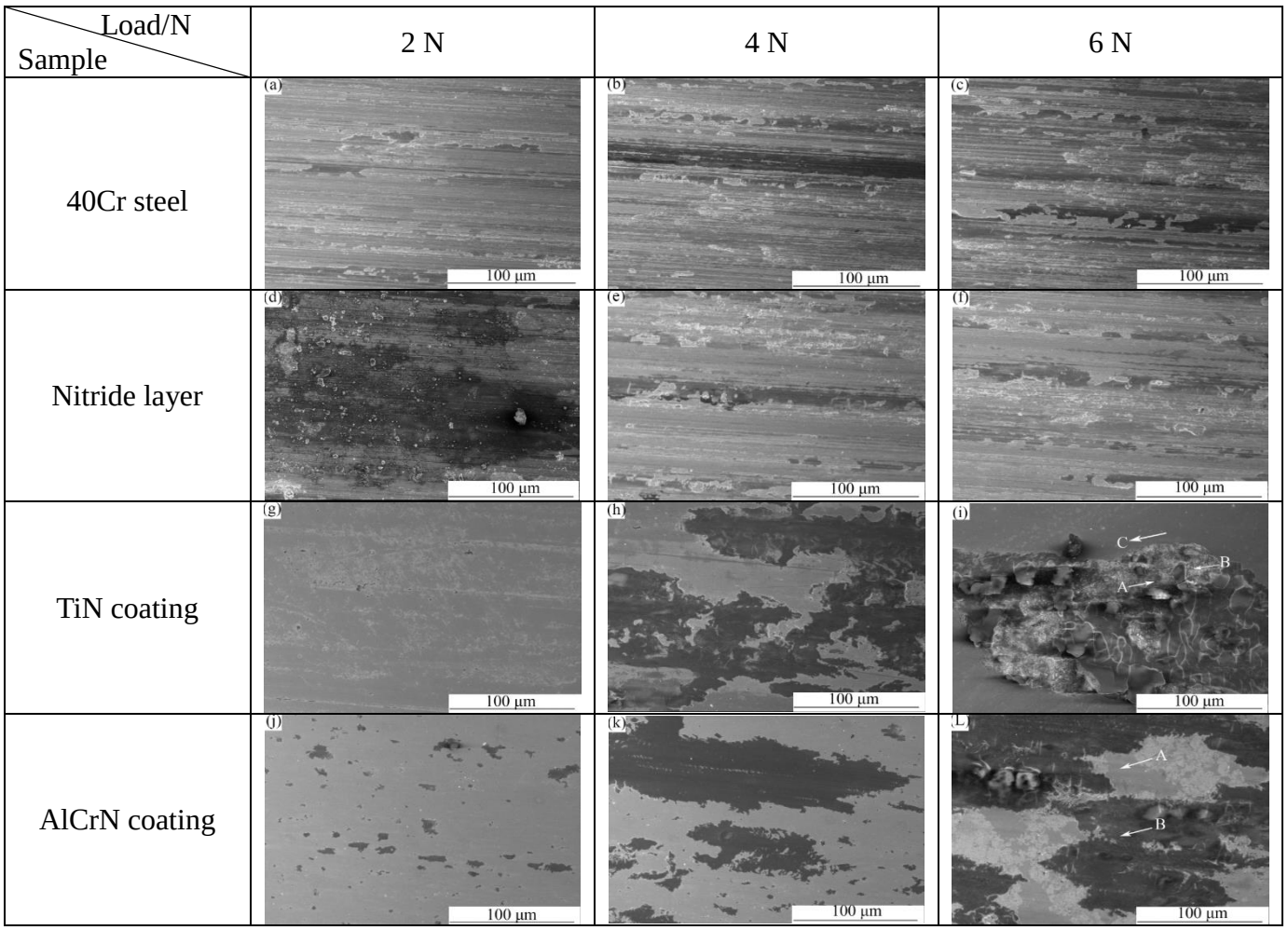

Figure 11. Morphologies of wear marks of 40Cr steel, nitride layer, TiN coating, and AlCrN coating, (a, b, c) Wear marks of the 40Cr steel under 2, 4, 6 N load; (d, e, f) Wear marks of the nitride layer under 2, 4, 6 N load; (g, h, i) Wear marks of TiN coating under 2, 4, 6 N load; (j, k, L) Wear marks of AlCrN coating under 2, 4, 6 N load. (The grinding pair selected Si_3N_4 ceramic ball diameter of 4 ㎜, load 2, 4, 6 N, test speed of 40 ㎜/s, the test duration is 1h, Magnification: 500x.)

Table 4. Elemental composition analysis of regions A, B and C in Figure 10 (i)

Composition	O/%	Ti/%	Fe/%	Si/%	Cr/%	N/%
A area	41.69	16.54	31.55	9.84	0.37	-
B area	22.41	7.14	66.13	3.78	0.55	-
C area	-	43.12	39.38	-	-	17.49

Table 5. Elemental composition analysis of regions A and B in Figure 10 (L)

Composition	O/%	Al/%	N/%	Fe/%	Cr/%	Si/%	Se/%
A area	-	8.51	11.17	78.17	2.85	-	-
B area	36.95	11.24	-	35.82	3.57	12.12	0.31

The wear mechanism of TiN coating and AlCrN coating is mainly adhesive wear. Figure 12 is the adhesion wear mechanism of coating. Figure 12(a) shows the friction between the ceramic ball and the coating forms the adhesion of micro-convex body, which is accompanied by the transfer of materials, and then forms the micro-convex body and continues to adhesion. It can be seen from Figure 12(b) that transfer groups are formed after material transfer. As we can see, Figure 12(c) shows that the transfer group is compressed again in the process of friction. Figure 12(d) shows more transfer groups are flattened and fall off in chunks, finally forming flake debris.

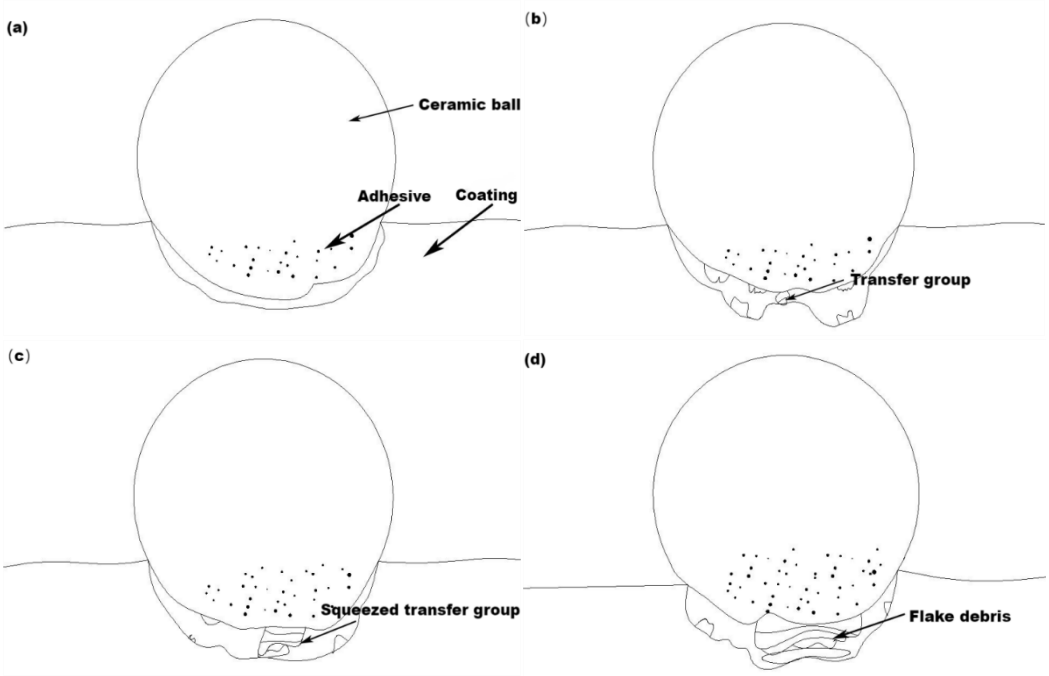

Figure 12. Adhesive wear mechanism of coating

Figure. 13 shows the wear rates of 40Cr steel, nitride layer, TiN coating and AlCrN coating. It can be seen from the figure that the wear rates of the four samples all increase with the increase of load. Under the same load, the wear rate of 40Cr steel is the highest, the wear rate of the nitride layer decreases, the wear rate of TiN coating and AlCrN coating decreases obviously, and the wear rate of AlCrN coating is the lowest. When the load is 2 N, the wear rate of the nitride layer, TiN coating and AlCrN coating decreases by 28.7%, 38.9% and 50.0%, respectively, compared with the 40Cr steel. At a load of 4N, the wear rate of the nitride layer, TiN coating, and AlCrN coating decreases by 38.5%, 51.8%, and 56.1% relative to the 40Cr steel, respectively. When the load is 6 N, the wear rate of the nitride layer, TiN coating and AlCrN coating decreases by 42.2%, 59.1% and 61.3%, respectively, compared with the 40Cr steel. The results show that the surface treatment methods of nitriding and nitriding combined with coating can improve the wear resistance of 40Cr steel, and the method of nitriding combined with AlCrN coating has the best effect, showing the excellent wear resistance of AlCrN coating.

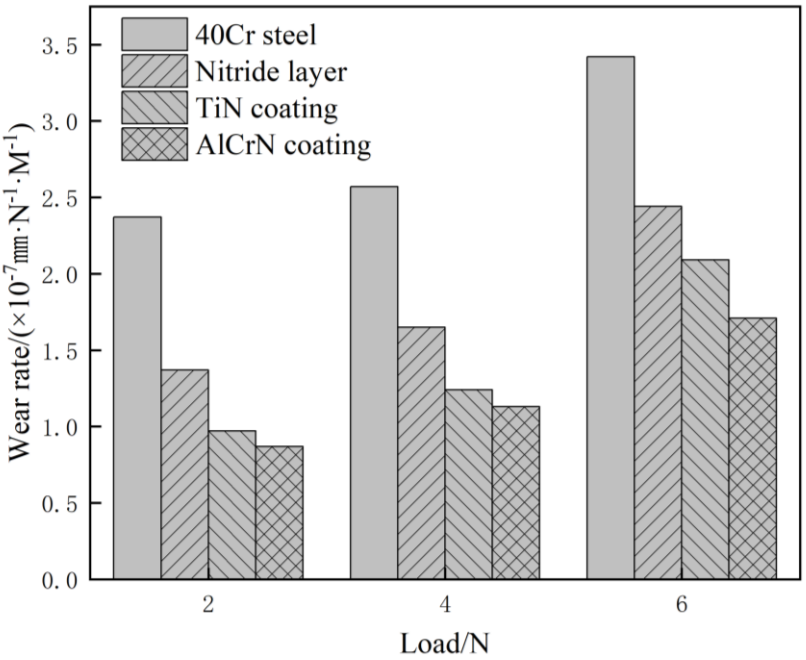

Figure 13. Wear rate diagram of 40Cr steel, nitride layer, TiN coating, and AlCrN coating. (The grinding pair selected Si_3N_4 ceramic ball diameter of 4 ㎜, load 2, 4, 6 N, test speed of 40 ㎜/s, the test duration is 1h.)

3.7 Corrosion behavior

Figure 14 shows the potentiodynamic polarization curve of 40Cr steel, nitride layer, TiN coating and AlCrN coating in 3.5% NaCl solution. The polarization curve is based on the change relationship between the corrosion current density and the electrode potential, so as to study the corrosion of the material corrosion resistance in the environment. Compared with the 40Cr steel, the curve of the nitride layer, TiN coating, and AlCrN coating is shifted positively, which may be due to the increase of cathode current and the decrease of anodic dissolution current, and the solution forms an adsorption barrier on the surface of samples to prevent the corrosion of the coating by the solution ions.[24] A smaller passivation region was found on the potentiodynamic polarization curve of the AlCrN coating, the passivation zone of the AlCrN coating starts at around -180 mV, indicating that the AlCrN coating can play a certain protective role, this is because the corrosion-resistant element Cr within the coating forms a dense passivation film that adsorbs Cl^-, thereby enhancing the corrosion resistance of the coating[25]. In the anode polarization of TiN coating, the current density increases with the increase of potential less than the increase rate of the matrix, this is due to he barrier layer with Ti layer could effectively inhibit the charge transfer between the coating and the matrix interface and improve the corrosion resistance of the coating.[9].

Corrosion potential (Ecorr) and corrosion current density (Icorr) characterize the corrosion resistance of the samples surface. After the polarization curve of composite coating was obtained, the potentiodynamic polarization curve was fitted using Tamry Echem Analyst software Tafel, and the

fitting results are shown in Table 6. Compared with the 40Cr steel, the Ecorr of the nitride layer, TiN coating and AlCrN coating increased by 9.6%, 24.2% and 42.6%, respectively, and the Icorr of the nitride layer, TiN coating and AlCrN coating decreased by 72.7%, 87.8% and 89.2%, respectively. According to electrochemical theory [26], the highest corrosion potential and the lowest corrosion current density indicate that the AlCrN coating has the best corrosion resistance, followed by the TiN coating, and the nitride layer has lower corrosion resistance than coatings but is better than 40Cr steel.

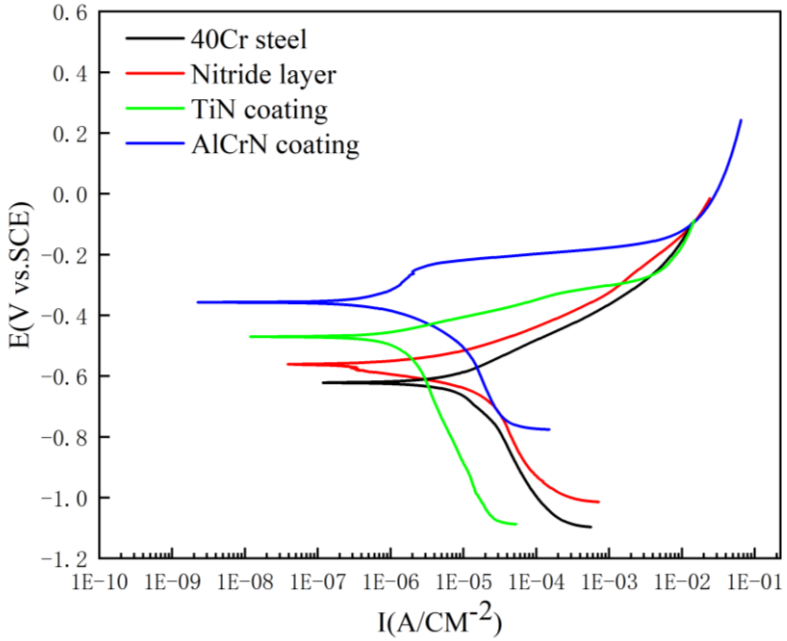

Figure 14. Potentiodynamic polarization curves of 40Cr steel, nitride layer, TiN coating and AlCrN coating in 3.5% NaCl solution. (The scanning potential is from -800 mV to -400 mV at 10 mV/s scanning rate.)

Table 6. Corrosion potential and corrosion current density polarization parameters of different samples

Sample	Icorr / μA·cm^{-2}	Ecorr / mV
40Cr steel	8.96	-622
Nitride layer	2.44	-562
TiN coating	1.09	-471
AlCrN coating	0.96	-357

4. CONCLUSIONS

Due to the solution strengthening effect of nitrogen atoms, nitriding can increase the hardness of the 40Cr steel to 520.4 $HV_{0.025}$. The coating prepared on the nitride layer forms the multi-layer coating. The hardness of TiN coating is increased to 1363.5 $HV_{0.025}$, and the hardness of AlCrN coating is increased to 2856.9 $HV_{0.025}$.The surface treatment methods of nitriding, nitriding combined with TiN

coating and nitriding combined with AlCrN coating can improve the wear resistance of 40Cr steel. The wear rate order from high to low is the 40Cr steel, nitride layer, TiN coating, and AlCrN coating. The wear mechanism of the 40Cr steel and nitride layer is mainly abrasive wear with slight adhesive wear. The adhesion of TiN coating and AlCrN coating is 26 N and 23 N respectively. The wear mechanism of TiN coating and AlCrN coating is mainly adhesive wear.The highest corrosion potential and the lowest corrosion current density indicate that the AlCrN coating has the best corrosion resistance, followed by the TiN coating, and the nitride layer has lower corrosion resistance than coatings but is better than 40Cr steel.

ACKNOWLEDGEMENTS
This research was financially supported by the Municipal University Cooperation Fund Project of Yangzhou (No. YZ2021151 and No. YZ2021155).

References

1. F.A. Guo,N. Trannoy,J. Lu, *Superlattice Microstruct*., 35(2004) 445–53.
2. X. Cheng, S. Hu, W.L. Song, X.S. Xiong, *Appl. Surf. Sci.*, 286 (2013) 334–343.
3. M. Morita, K. Hasegawa, S. Motoda, *ISIJ Int.*, 60.11(2020) 2525.
4. F. Bahremandd, T. Shahrabi, B. Ramezanzadeh, *J. Hazard. Mater.*, 403(2020) 123722.
5. H.Q. Sun, Y.N. Shi, M.X. Zhang, K. Lu, *Surf. Coat. Techno*, 202.16(2008)3947-53.
6. Z.H. Kou, M.L. Bai, H.W. Yang , *Adv Mat Res*., 648(2013) 202-205.
7. S. Ramesh, S. Natarajan, V.J. Sivakumar. *Surf. Eng. Appl. Electrochem.*, 56.3(2020):301-310.
8. A. Soni, W. Trojahn,M. Dinkel, T.Hosenfeldt, *Trans. Indian Inst. Met*., 74.5(2021):1231-1239.
9. F.Y. Ouyang, W.L. Tai, *Appl. Surf. Sci.*, 276(2013)563-570.
10. M.F. Gong, J. Chen, X. Deng, S.H. Wu, *Int J Refract Hard Met*., 69 (2017)08003.
11. J.W. Du, L. Chen, J. Chen, Y.Du, *Vacuum.*, 179 (2020)109468..
12. F. Zhou, K.M. Chen, M.L. Wang, X.J. Xu, H. Meng, M. Yu, Z.D. Dai, *Wear.*, 265.7-8(2008) 1029-1037.
13. J.C.A. Batista, C. Godoy, A. Matthews, *Tribol Int*., 35(2002)363-372.
14. Y.H. Zhao, B.H. Yu, L.M. Dong, H. Du, J.Q. Xiao, *Surf. Coat. Technol.*, 210(2012)90-96.
15. C. Zhao, C.X. Li, H. Dong, T.Bell, *Surf. Coat. Techno.*, 201(2006) 2320-2325.
16. S. Ramesh, S. Natarajan, V.J.Sivakumar , *Surf. Coat. Techno.*, 56.3(2020):301-310.
17. J.L. Mo, M. H. Zhu., *Wear.*, 267(2009) 874-881.
18. A. Schneider, D. Steinmueller-Nethl, M. Roy, F. Franek, *Int J Refract Hard Met.*, 28.1(2010):40-50.
19. G.S. Fox-Rabinovich, K. Yamamoto, A.I. Kovalev, S.C. Veldhuis, L.Ning, L.S.Shuster, A. Elfizy, *Surf. Coat. Technol.*, 202.10(2008)2015-2022.
20. X.R. Ren, Z. Huang, M.X. Liu, J.G.Yang, H. Chen, *Rare Metal Mat Eng.*,47.4 (2018)1100-1106 .
21. L. Yang, G.G. Cheng, S.J. Li, M. Zhao, G.P. Feng, T. Li, *Int. J. Miner. Metall. Mater.*, 22.12(2015)1266－1272.
22. A.Y. Adesina, Z.M Gasem, F.A. Al-Badour, *J Manuf Process.*, 25(C)(2017) 432－442.
23. Y.C. Chim, X.Z. Ding, X.T. Zeng, S. Zhang, *Thin Solid Films.*, 517.17(2009) 4845-4849.
24. M.L. Ban, K.D. Li, Q.S. Tao, A.L. Fan, B. Tang, J.Q. Zhang, *Int. J. Electrochem. Sci*., 16 (2021) 210562

25. D.S. Li, K. Chen, X.Q. Fu, M. Kang, Z.X. Hua,X.F. Wang, *Int. J. Electrochem. Sci*., 16 (2021) 210233
26. H. Wang, J. Liu, D.W. Gu, D. Zhu, Int. *J. Electrochem. Sci*., 15 (2020) 9313.